Crystallographic and magnetic structure of ZnV_2O_4

Structural phase transition due to spin-driven Jahn-Teller distortions

M. Reehuis[1,a], A. Krimmel[1,b], N. Büttgen[1], A. Loidl[1], and A. Prokofiev[2]

[1] Experimentalphysik V, Elektronische Korrelationen und Magnetismus, Institut für Physik, Universität Augsburg, 86159 Augsburg, Germany
[2] Physikalisches Institut, Johann Wolfgang Goethe-Universität, 60054 Frankfurt, Germany

Abstract. We report on the crystallographic and magnetic structure of the geometrically frustrated spinel ZnV_2O_4 as determined by neutron powder diffraction. At $T = 51$ K, a cubic-to-tetragonal phase transition takes place. The low temperature crystallographic structure is characterized by the space group $I4_1/amd$ and unit cell dimensions $a/\sqrt{2} \times a/\sqrt{2} \times a$ with a being the lattice constant of the cubic phase. The corresponding antiferromagnetic structure of the vanadium sublattice can be described by a propagation vector $\mathbf{k} = (001)$ with the magnetic moments being aligned parallel to the c-axis. The ordered magnetic moment is 0.65(5) μ_B per V^{3+} ion. The experimental results are in accord with recent theoretical models proposing spin-driven Jahn-Teller distortions. The results are also compared with reports on non-ordering ZnV_2O_4.

1 Introduction

At room temperature, ZnV_2O_4 is a Mott insulator crystallizing in the cubic normal spinel structure. The V^{3+} ions ($S = 1$) occupying the B-sites of the AB_2O_4 structure form a corner-sharing tetrahedral network and are octahedrally coordinated by six oxygen ions. Tetrahedral networks of localized spins often are governed by strong geometrical frustration and reveal fascinating ground states [1] like a spin liquid [2] or a spin ice [3,4]. Magnetic measurements revealed that ZnV_2O_4 orders magnetically below $T_N = 40$ K [5,6]. The paramagnetic behaviour is rather anomalous and the Curie-Weiss temperature, as well as the paramagnetic moment strongly depend on the range of the data analysis [5,6,9]. Curie-Weiss temperatures ranging from -400 K to -1000 K have been reported. The enormous difference between the Curie-Weiss temperature and the Néel temperature has been attributed to frustration effects. However, as indicated above, non-trivial or disordered ground states are expected in a strongly frustrated system while ZnV_2O_4 reveals a simple antiferromagnetic phase. A cubic-to-

tetragonal structural phase transition at $T_S = 51$ K has been reported by Ueda *et al.* [6] which precedes the magnetic phase transition and removes frustration effects thus making long range antiferromagnetic order favorable. The cubic-to-tetragonal phase transition is evidenced by a typical peak splitting in the X-ray diffraction pattern with a tetragonal distortion $c/a \approx 0.994$ [6]. A lattice distortion with $c/a < 1$ is rather unusual and indicates that the oxygen octahedra around the vanadium interstices shrink along c but are elongated within the a, b-plane. In this case, the t_{2g} levels split into a lower d_{xy} singlet and higher d_{yz} and d_{xz} doublets and only one of the two t_{2g} electrons of the V^{3+} ions can lower its energy. It has been pointed out by Rogers *et al.* [7] that in the case of a V^{3+} interstice and a non-collinear spin arrangement a tetragonal Jahn-Teller distortion with $c/a < 1$ is expected. Recently, similar conclusions have been derived by Kondo *et al.* [8], however based on a X-ray study of the isostructural compound MgV_2O_4 which reveals a very similar structural and magnetic behaviour. In MgV_2O_4, the cubic-to-tetragonal distortion ($T_S = 65$ K, $c/a = 0.993$) is followed by an antiferromagnetic transition at $T_N = 42$ K [9,10]. In CdV_2O_4, these transitions take place at 97 K and 35 K, respectively and the tetragonal distortion is $c/a = 0.990$ [11,12].

[a] *Present address:* Hahn-Meitner-Institut, Glienicker Str. 100, 14109 Berlin, Germany
[b] e-mail: `alexander.krimmel@physik.uni-augsburg.de`

The magnetic structure of ZnV_2O_4 at $T = 4.2$ K has been determined by Nizioł on the basis of neutron powder diffraction almost three decades ago [5]. It was concluded that antiferromagnetic ordering of the vanadium magnetic moments appears along [110] and [1$\bar{1}$0] when indexed in the cubic spinel structure. The spins are aligned along the [001] direction with a saturated ordered magnetic moment of 0.8(3) μ_B. However, it should be clearly stated that the counting statistics of the magnetic Bragg reflections was rather low and the magnetic structure could only be determined assuming the known antiferromagnetic structure of MgV_2O_4.

Theoretical models to explain the ground state properties of spinels with magnetic ions at the B-site exist since long [13]. An explanation of the structural phase transition of ZnV_2O_4 has been given by Yamashita and Ueda [14] in terms of a spin-driven Jahn-Teller distortion. This model naturally explains the rather low structural transition temperature and the fact that it is slightly higher than the magnetic ordering temperature, as well as accounting for the particular kind of distortion ($c/a < 1$). This spin-driven Jahn-Teller distortion of ZnV_2O_4 has in turn consequences onto the magnetic coupling and the possible magnetic structures [14]. Additionally, the temperature dependence of the magnetic susceptibility and electronic entropy could also been accounted for [14].

Despite of being of utmost importance for any sound physical interpretation, to our knowledge the low temperature crystallographic and magnetic structures of ZnV_2O_4 have not been established rigorously. Many of the conclusions were derived relying on experimental facts from MgV_2O_4. In order to provide a solid structural basis for the unusual physical properties of ZnV_2O_4, we have performed a series of neutron powder diffraction experiments and studied in detail the low-temperature nuclear and magnetic structure.

2 Experimental details

Polycrystalline material of ZnV_2O_4 was prepared by a solid state reaction of V_2O_3 (Chempur, 99,9%) and ZnO (Alfa Aesar, 99,99%). Before the synthesis, commercial V_2O_3 was annealed at 750 °C in a H_2 (5%)/Ar-stream during 1 day. A fine mixture of binary oxides was pressed into pellets and sealed in a silica ampoule filled with argon. After slow temperature increase the samples were annealed stepwise from 700 °C to 900 °C during 17 days with three intermediate grindings. At room temperature, X-ray powder diffraction of ZnV_2O_4 confirmed the cubic spinel structure without any impurity phases. The unit cell parameter as deduced from the Rietveld fit is $a = 8.401$ Å.

The magnetic properties of ZnV_2O_4 were measured employing a superconducting quantum interference device (Quantum Design MPMS) in the temperature range $1.8 \leq T \leq 400$ K and fields up to 5 T. Neutron powder diffraction patterns of ZnV_2O_4 for $T = 1.8$ K, 60 K and $T = 70$ K were collected on the instruments E6 and E9 at the BERII reactor of the Hahn-Meitner-Institut, Berlin. The instrument E6 uses the (0 0 2) reflection of a double

focusing graphite monochromator resulting in an incident neutron wavelength of $\lambda = 245.0$ pm. The instrument E9 is equipped with a germanium monochromator selecting the wavelength $\lambda = 179.8$ pm. Data sets were recorded for an angular range $5° \leq 2\theta \leq 85°$ on E6 and $5° \leq 2\theta \leq 150°$ on E9, respectively. The crystallographic and magnetic structure of ZnV_2O_4 was refined from the powder diffraction data by standard Rietveld analysis employing the program FULLPROF [15]. For the refinement, the nuclear scattering lengths $b(Zn) = 5.68$ fm, $b(V) = -0.3824$ fm and $b(O) = 5.805$ fm were used [16]. The magnetic form factors of V^{3+} were taken from reference [17]. Additional weak reflections could be observed in the powder pattern at around 45° and 53°. These intensities can be ascribed to scattering from the aluminum of the cryostat.

3 Experimental results and discussion

3.1 Magnetic properties

Field cooled (FC) and zero-field cooled (ZFC) susceptibilities of ZnV_2O_4 as measured in an external field of 10 Oe are shown in Figure 1. The structural phase transition at $T_S = 51 \pm 1$ K and the antiferromagnetic transition at $T_N = 40 \pm 2$ K are clearly visible. The absence of any pronounced Curie tails at low temperatures, even in this low measuring field signals the absence of paramagnetic impurities and demonstrates the high quality of the sample. The results are very similar to those reported by Ueda *et al.* [6]. However, in our measurements the splitting of the FC and ZFC susceptibility appears just above T_S, significantly lower than observed in reference [6]. We interpret this splitting as being due to magnetic fluctuations and believe that it does not represent a characteristic temperature.
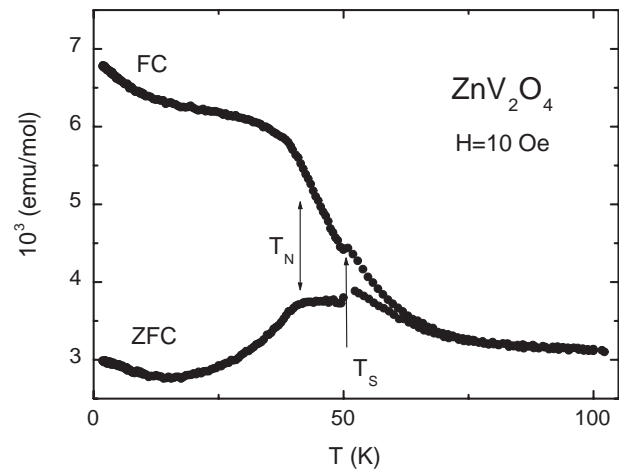
Fig. 1. Field cooled (FC) and zero-field cooled (ZFC) magnetic susceptibilities of ZnV_2O_4 in an external field of 10 Oe. The structural and magnetic phase transitions at $T_S = 51 \pm 1$ K and $T_N = 40 \pm 2$ K, respectively are indicated by arrows.
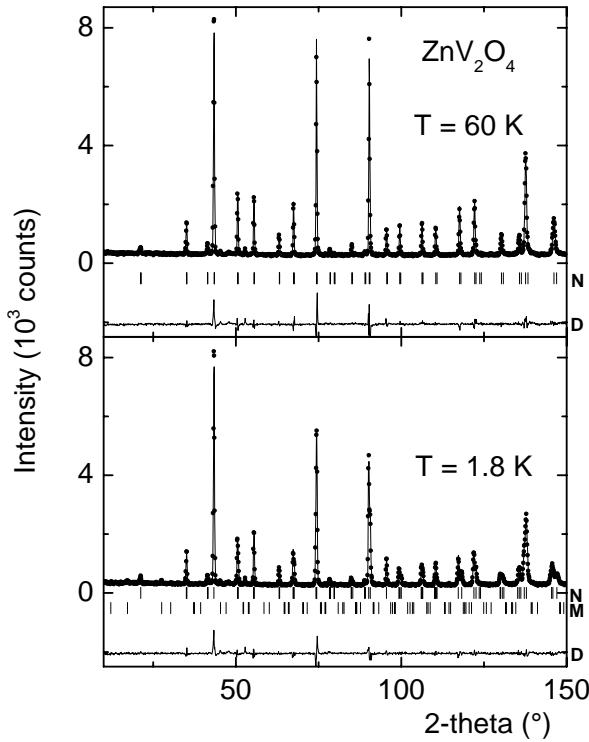
Fig. 2. Neutron powder diffraction patterns and corresponding Rietveld refinement of ZnV_2O_4 at $T = 60$ K (upper panel) and $T = 1.8$ K (lower panel). Shown are the observed (full circles) and calculated (full lines) intensities, the difference between observed and calculated intensities (bottom line labelled D) and the peak positions (vertical bars) of the nuclear (label N) and magnetic (label M) structure.

3.2 The crystallographic structure of ZnV_2O_4

The crystallographic structure of ZnV_2O_4 was determined from the neutron powder diffraction data collected on the instrument E9 at 1.8 K and at 60 K, respectively. Corresponding diffraction patterns of ZnV_2O_4 are shown in Figure 2.

At $T = 60$ K, the compound crystallizes in the cubic spinel structure characterized by space group $Fd\bar{3}m$. The atoms Zn, V and O are located on the Wyckoff positions $8a$ (1/8, 1/8, 1/8), $16d$ (1/2, 1/2, 1/2) and $32e$ (x, x, x), respectively. At $T_s = 51$ K, a structural phase transition takes place. The low temperature phase is of tetragonal symmetry described by space group $I4_1/amd$. At $T = 1.8$ K, the tetragonal unit cell is just one half of the cubic one with cell dimensions $a/\sqrt{2} \times a/\sqrt{2} \times a$. In this structure, the atoms Zn, V and O are found on the Wyckoff positions $4a$ (0, 3/4, 1/8), $8d$ (0, 0, 1/2) and $16h$ $(0, x, z)$, respectively. During the refinements, a total of 9 (for $T = 60$ K) and 10 (for $T = 1.8$ K) parameters were allowed to vary: An overall scale factor, 5 peak-shape parameters, the occupation number of oxygen, the isotropic thermal factor B of Zn and O respectively, as well as one (for $T = 60$ K) or two (for $T = 1.8$ K) positional parameters of oxygen. The Rietveld refinements of the crystallographic structures resulted in residuals of 0.047 for the

Table 1. The nuclear and magnetic structure of ZnV_2O_4 as obtained by Rietveld refinements from neutron powder diffraction data. Listed are the lattice constants a and c, the corresponding unit cell volume V, the oxygen positional parameters in fractional coordinates, the isotropic temperature factors, the ordered magnetic moment and the residuals of the refinements. The isotropic thermal parameters of vanadium were kept fixed during the refinements. R_N is the residual of the nuclear structure defined as $R_N = \Sigma |F_o - F_c|/\Sigma F_o$.

ZnV_2O_4	$I4_1/amd$	$Fd\bar{3}m$
T (K)	1.8	60
a (Å)	5.9526(4)	8.4028(4)
c (Å)	8.3744(6)	
V (Å^3)	296.73(6)	593.30(8)
x(O)	-	0.2604(2)
x(O)	0.0200(5)	-
z(O)	0.2611(5)	-
B_{Zn} (Å^2)	0.20(15)	0.49(17)
B_V (Å^2)	0.2	0.2
B_O (Å^2)	0.29(9)	0.45(6)
R_N (No. of F's)	0.032(51)	0.047(20)
Data taken on E6		
μ_{exp}(V) (μ_B)	0.61(5)	-
R_M	0.078	-
Data taken on E9		
μ_{exp}(V) (μ_B)	0.65(5)	-
R_M	0.040	-

cubic and 0.032 for the tetragonal phase, respectively. The results are summarized in Table 1.

The six-fold coordinated V^{3+} ions are in the center of oxygen octahedra. In the high-temperature ($T \geq 51$ K) cubic form of ZnV_2O_4, the vanadium-oxygen distance is identical for all 6 oxygen atoms (d(V-O) = 2.0168 Å). In contrast, the distance between the vanadium and the apical O-atom which is approximately parallel to the c-axis, is shortened in the low-temperature tetragonal phase (d(V-O) = 2.0041 Å). On the other hand, the distance of the 4 equatorial O-atoms (approximately within the ab-plane) becomes larger (d(V-O) = 2.0243 Å). The Jahn-Teller distortion of these oblate octahedra is thus

$d(\text{V-O}_{apical})/d(\text{V-O}_{equatorial}) = 0.990$ and is at the origin of this structural phase transition. The corresponding tetragonal distortion $c/a = 0.99480(12)$ is in excellent agreement with reference [6], however, significantly smaller than the octahedral distortion. It is interesting to note that the unit cell volume in the tetragonal phase at $T = 1.8$ K $2V_{tetragonal} = 593.46(12)$ Å^3 (doubled tetragonal cell) is, within the experimental uncertainties, identical to the unit cell volume at $T = 60$ K in the cubic phase, $V_{cubic} = 593.30(12)$ Å^3, indicating that the cubic-to-tetragonal phase transition is volume conserving.

3.3 The magnetic structure of ZnV$_2$O$_4$

The neutron powder diffraction pattern collected at $T = 1.8$ K revealed weak additional reflections which could be unambiguously ascribed to the onset of long range magnetic order of the vanadium sublattice. The two strongest magnetic Bragg peaks could be indexed as $(1, 0, 0)_M$ and $(1, 1, 1)_M$. Thus, the magnetic structure violates the I-centering and the reflections can be generated by the rule $(hkl)_M = (hkl)_N + \mathbf{k}$ where the propagation vector $\mathbf{k} = (0, 0, 1)$ is an invariant vector on the surface of the Brillouin zone [18]. The vanadium atoms are located at the Wyckoff position $8d$ of the space group $I4_1/amd$. Our data analysis showed that two spin configurations are possible to account for the intensities of the main magnetic reflections. The atoms numbered as V1: $(0, 0, {}^1/_2)$, V2: $(0, {}^1/_2, {}^1/_2)$, V3: $({}^1/_4, {}^1/_4, {}^1/_4)$ and V4: $({}^1/_4, {}^3/_4, {}^3/_4)$ can show either a spin sequence $+ - - -$ (type 1) or $+ - + +$ (type 2) with a moment direction parallel to the $c-$axis. The two strongest magnetic Bragg reflections are barely visible in the low temperature diffraction pattern, as shown in Figure 2. To convince the reader that long-range magnetic order really does exist in ZnV$_2$O$_4$ a limited angular range has been remeasured with high statistical accuracy on the diffractometer E6. The data around the two strongest magnetic Bragg reflections in the paramagnetic ($T = 70$ K) and in the antiferromagnetic phase ($T = 2$ K) are shown in Figure 3 and unambiguously demonstrate the onset of long range magnetic order. The refined ordered magnetic moment of the vanadium ions are $\mu_{exp} = 0.61(5)$ μ_B and $\mu_{exp} = 0.65(5)$ μ_B as obtained from the data sets recorded on the two different instruments E6 and E9, respectively. The observed and calculated magnetic intensities are listed in Table 2.

The magnetic structure of ZnV$_2$O$_4$ is shown in the left panel of Figure 4 and is different as reported previously [5]. Crystallographically, one finds edge-sharing octahedra both along the a- and b-axis. Along these directions, the magnetic moments form antiferromagnetic spin sequences according to $+ - + - ...$ whereas they are ferromagnetically aligned along c. The magnetic structure of type 2 is very similar. Here the only difference arises from a spin inversion of the moments in the antiferromagnetic chain going along the a-axis.

The crystallographic and magnetic phase transitions in ZnV$_2$O$_4$ have recently been explained in terms of a
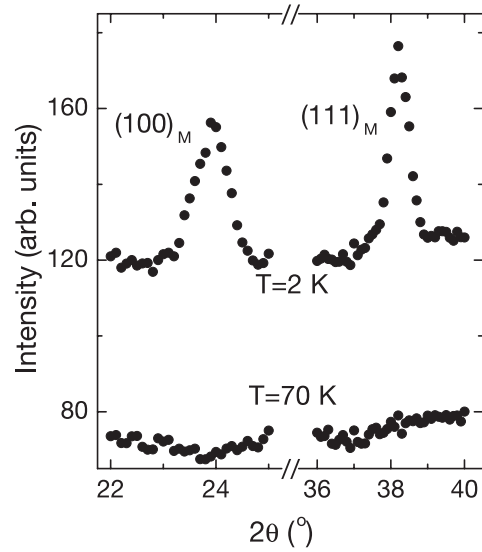

Fig. 3. Neutron powder diffraction data of ZnV$_2$O$_4$ at $T = 70$ K (lower part) and $T = 2$ K (upper part) evidencing the presence of the $(100)_M$ and $(111)_M$ magnetic Bragg reflections at low temperatures.

Table 2. Observed and calculated magnetic intensities of ZnV$_2$O$_4$ derived from measurements on two different diffractometers.

hkl	I_{calc}	E6 ($\lambda = 2.450$ Å)		E9 ($\lambda = 1.798$ Å)	
		I_{obs}	2θ	I_{obs}	2θ
001	0	0	16.81	0	12.33
100	97	111	23.73	100	17.38
111	100	100	37.98	100	27.66
102	16	13	41.89	15	30.44
201	0	0	51.75	0	37.40
003	0	0	52.03	0	37.58
210	22	20	54.74	29	39.48

spin-driven Jahn-Teller effect [14,19,20]. Given a magnetoelastic coupling of a degenerate spin system, the magnetic energy may be reduced by a lattice distortion. As the magnetic energy reduction is linearly dependent on the atomic displacements, whereas the cost of elastic energy depends quadratically on the displacements, a Jahn-Teller distortion results from the spin degeneracy. Yamashita and Ueda [14] discussed such a spin-driven Jahn-Teller distortion for a single tetrahedron of spins $S = 1/2$. Tchernyshyov, Moessner and Sondhi [19,20] extended this analysis to the case of the infinite pyrochlore
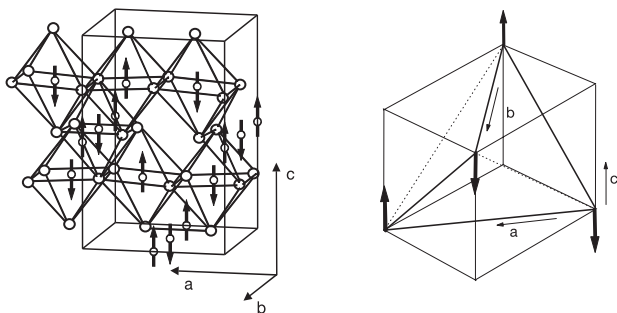
Fig. 4. Left panel: The corresponding magnetic structure of ZnV$_2$O$_4$ as determined on the basis of the Rietveld refinements. The magnetic moments of the V^{3+} ions being located on the axis of the unit cell are shown without oxygen octahedra for the sake of clarity. These atoms are included to illustrate the antiferromagnetic spin sequence along the *b*-axis. The figure also evidences the buckling of the VO$_6$ octahedra. Right panel: A single tetrahedron of the corner-sharing tetrahedral network of magnetic vanadium ions of ZnV$_2$O$_4$. The axis labels refer to the tetragonally distorted low-temperature structure. The full and dotted lines of the tetrahedron refer to strong and weak bonds of neighboring spins, respectively, according to references [19,20] (see text).

lattice with arbitrary spin, accounting for the various possible distortions and corresponding spin configurations. The structural distortion leads to bond ordering in the spin system. In the present case of ZnV$_2$O$_4$ we have 4 strong and 2 weak bonds per tetrahedron, indicated by full and dotted lines in Figure 4, respectively. The corresponding magnetic structure (taking place at a somewhat lower temperature) is a collinear spin arrangement shown by the arrows of Figure 4.

4 Conclusion

In the present work we have unambiguously determined the low-temperature structural and magnetic properties of ZnV$_2$O$_4$. At $T = 51$ K, ZnV$_2$O$_4$ transforms from a cubic high-temperature phase ($Fd\bar{3}m$) into a tetragonal low-temperature phase ($I4_1/amd$) with $c/a = 0.9948$. Passing through the phase transition, the t_{2g} levels split into a d_{xy} singlet and an excited d_{xz}/d_{yz} doublet and only one of the two t_{2g} electrons can lower its energy. This rather unusual ground state with $c/a < 1$ can be explained assuming a spin-driven Jahn-Teller effect as recently proposed by Yamashita and Ueda [14] and subsequently elaborated in more detail by Tchernyshyov *et al.* [19,20]. The structural phase transition relaxes the frustration effects and at 42 K ZnV$_2$O$_4$ reveals antiferromagnetic order with an ordered magnetic moment of 0.63 μ_B.

It is well known that the physical properties of ZnV$_2$O$_4$ sensitively depend on sample preparation conditions. A slightly different heat treatment results in single phase material of the proper stoichiometry and normal spinel-type crystal structure of ZnV$_2$O$_4$ at room temperature, but without indications of a structural phase transition. The cubic spinel structure is thus preserved down to low

temperatures and, consequently, the inherent geometrical frustration prevents long range magnetic order as evidenced by the absence of magnetic Bragg reflections in neutron powder diffraction measurements [21]. That indeed ZnV$_2$O$_4$ is very close to a structural instability is supported by recent and ongoing *ab initio* calculations [22] which demonstrate that the ground state depends very sensitively on the lattice constant and oxygen coordinate x.

To obtain insight into the magnetically disordered ground state properties of this type of ZnV$_2$O$_4$, μSR studies have been performed [21,23]. The μSR spectroscopy on ZnV$_2$O$_4$ revealed a purely paramagnetic state above 40 K. For $12 \leq T \leq 40$ K, the paramagnetic state coexists with a dynamically correlated spin-glass-like state whose volume fraction increases as temperature is reduced, reaching 100% around 12 K. Below 12 K, a strongly damped Bessel-type oscillatory behaviour indicates an incommensurate spin-density-wave-like structure. The high transverse relaxation rate corresponds to a large local spin disorder preventing the onset of true long range magnetic order that explains the absence of magnetic Bragg reflections in neutron powder diffraction experiments. Furthermore, persistent slow spin fluctuations are observed. These features are indicators of strong frustration effects, leading to a highly correlated, but also highly disordered dynamic magnetic ground state in cubic ZnV$_2$O$_4$ [21,23]. Hence, ZnV$_2$O$_4$ belongs to the rare examples where a Jahn-Teller distortion appears at low temperatures, which can easily be suppressed and ZnV$_2$O$_4$ can be studied with an antiferromagnetic and a disordered ground state.

References

1. For a review, see for example: R. Moessner, Can. J. Phys. **79**, 1283 (2001)
2. B. Canals, C. Lacroix, Phys. Rev. B **61**, 1149 (2000)
3. A.P. Ramirez, A. Hayashi, R.J. Cava, R. Siddharthan, B.S. Shastry, Nature **399**, 333 (1999)
4. S.T. Bramwell, M.J.P. Gingras, Science **294**, 1495 (2001)
5. S. Nizioł, Phys. Stat. Sol. A **18**, K11 (1973)
6. Y. Ueda, N. Fujiwara, H. Yasuoka, J. Phys. Soc. Jpn **66**, 778 (1997)
7. D.B. Rogers, R.J. Arnott, A. Wold, J.B. Goodenough, J. Phys. Chem. Solids **24**, 347 (1963)
8. S. Kondo, C. Urano, Y. Kurihara, M. Nohara, H. Takagi, J. Phys. Soc. Jpn **69**, Suppl. B 139 (2000)
9. H. Mamiya, M. Onoda, Sol. State Comm. **95**, 217 (1995)
10. H. Mamiya, M. Onoda, F. Furubayashi, J. Tang, I. Nakatani, J. Appl. Phys. **81**, 5289 (1997)
11. N. Nishiguchi, M. Onoda, J. Phys.: Condens. Matter **14**, L551 (2001)

12. M. Onoda, J. Hasegawa, J. Phys.: Condens. Matter **15**, L95 (2003)
13. J. Villain, Z. Phys. B **33**, 31 (1979)
14. Y. Yamashita, K. Ueda, Phys. Rev. Lett. **85**, 4960 (2000)
15. J. Rodriguez-Carvajal, Physica B **192**, 55 (1993)
16. V.F. Sears, in: *International Tables of Crystallography,* edited by A.J.C. Wilson, Vol. C (Kluwer, Dordrecht, 1992), p. 383
17. P.J. Brown, in: *International Tables of Crystallography,* edited by A.J.C. Wilson, Vol. C (Kluwer, Dordrecht, 1992), p. 391
18. E.F Bertaut, J. Phys. France Colloq., Suppl. 2-3, C1-462 (1972)
19. O. Tchernyshyov, R. Moessner, S.L. Sondhi, Phys. Rev. Lett. **88**, 067203 (2002)
20. O. Tchernyshyov, R. Moessner, S.L. Sondhi, Phys. Rev. B **66**, 064403 (2002)
21. N. Büttgen, A. Krimmel, A. Loidl, M. Klemm, S. Horn, D.R. Noakes, E. Schreier, G.M. Kalvius, Physica B **312-313**, 703 (2002)
22. R. Valenti, private communication
23. G.M. Kalvius, D.R. Noakes, R. Wäppling, N. Büttgen, A. Krimmel, M. Klemm, S. Horn, A. Loidl, Physica B **326**, 470 (2003)